# STUDY OF THE CHEESE SALTING PROCESS BY DIELECTRIC PROPERTIES AT MICROWAVE FREQUENCIES

**J. Velázquez-Varela[1], M. Castro-Giraldez*[1], L. Cuibus[2], J.A. Tomas-Egea[1], C. Socaciu[2], P.J. Fito[1]**

[1]Instituto Universitario de Ingeniería de Alimentos para el Desarrollo, Universitat Politècnica de València, Camino de Vera s/n, 46022 Valencia, Spain

[2] University of Agricultural Sciences and Veterinary Medicine, Mănăştur Street, 3-5, 400372, Cluj-Napoca, Romania

*Author for correspondence: marcasgi@upv.es

## Abstract

Salting process involves complex phenomena that affect the overall quality of cheese because of its effect on water activity and induced biochemical changes. Permittivity of cheese was analysed throughout cheese salting treatment in order to relate it with water and salt transports. Salting treatment was carried out by using 25% (w/w) sodium chloride brine at 4ºC. Samples were immersed in a vessel containing the osmotic solution with continuous stirring, for 0, 10, 20, 30, 40, 50, 60, 90, 120, 180, 240, 360, 480, 720, 900 and 1440 min. Samples were subsequently equilibrated in an isothermal chamber at 4ºC for 24 hours. Mass, volume, surface water activity, moisture, ion content and permittivity were determined in fresh and salted samples. Permittivity was measured from 500 MHz to 20 GHz, by using an open-ended coaxial probe connected to a Vector Network Analyzer. Results showed that measurements at 20 GHz explain the water loss and water flux in the overall product. The state of the electrolytes in cheese can be followed using the ionic conductivity at 500 MHz. A coupled measurement of permittivity at 20 GHz and 500 MHz can predict the chemical species involved in cheese salting process, and its

structural changes. In conclusion, measures of permittivity in microwaves range can be used to monitor the salting cheese process.

**Keywords:** cheese, brining, permittivity, sodium chloride

## 1. Introduction

Cheese production is a complex process, which involves different units operations and biochemical transformations (Walstra et al., 2006). The salting treatment is an important operation in the manufacture of cheese; the salt normally used is sodium chloride (NaCl), which serves to many purposes: to improve the flavour, texture and colour of cheese, but it is also meant to kill off the starter cultures used in the cheese-making process, preventing further growth and the development of acid. In addition, it helps to reduce the water activity that prevents the growth of undesirable microorganisms (Aly & Galal, 2002; Abdalla and El-Zubeir, 2006).

Cheese consists on a matrix of protein, with fat and water components as an emulsion (Dickinson & Miller, 2001; Green, 1997). Essentially the matrix is composed of overlapping and cross-linked strands, mainly composed of casein aggregates; the integrity of the matrix is maintained by various intra- and inter-aggregate hydrophobic and electrostatic attractions (Fox et al., 1996). The addition of salt in cheese affects its functional characteristics (Floury et al., 2009), principally in the protein hydration and in the modification of the water binding capacity of casein within the cheese matrix, affecting the stability properties (Mamdouh, 2012).

The salting process is commonly performed using brines, where the control of NaCl content is very important to determine the physicochemical characteristics of cheese. It is

necessary to obtain a technique that allows determining, in a rapid and easy way, the salt content in cheese; this still remains as an unsolved problem in the food industry (Chevalier et al., 2006). In this sense, microwave dielectric spectroscopy could be an interesting technique to monitor salting process. This technique has been already used for monitoring the salting meat process (Castro-Giráldez et al., 2010). Some authors determined the dielectric properties of salted and unsalted butter over the MW frequency range (Ahmed et al., 2007; Shiinoki et al., 1998). Moreover, this technique have been already used in the analysis of cheese composition and cheese maturity (Ball et al., 1996; Cevoli et al., 2012; Everard et al., 2006; Green, 1997; Herve et al., 1998; Kubiš et al., 2001; Smith et al., 2011).

Complex permittivity (ε*) describes the behaviour of a food when subjected to an external electric field (Nelson & Datta, 2001). The two components of complex permittivity (ε' and ε'') are called dielectric constant and loss factor, respectively. The dielectric constant represents the real part of complex permittivity, and is related to the material ability to store energy; the loss factor represents the imaginary part, which is related to the absorption and dissipation of the electric energy in other kinds of energy, such as thermal or mechanical (Castro-Giráldez et al., 2010; Schwan, 1988).

In the range of microwaves, the interaction of the electric field with foods produces two main effects, γ-dispersion and ionic conductivity. The first one is caused by dipolar molecules orientation and induction, and it is produced at GHz frequencies (Mohiri et al., 2011). The other important effect in microwave range is ionic conductivity; the application of an electric field causes the vibration of food ions (Metaxas and Meredith, 1983) increasing the internal energy of the molecules.

The aim of the present study is to obtain and analyse the dielectric properties of cheese during the salting process and to assess the potential use of dielectric spectroscopy to monitor this process.

## 2. **Material and Methods**

### 2.1 Raw material

18 cheeses were proportionated by Formatgeria Granja Rinya S.L. factory (Valencia, Spain). All the cheeses were of the fresh Tronchon type and they were conducted under the same pressing conditions and with identical compositional characteristics. The cheeses were provided unsalted and just after the pressing operation. Samples were obtained from the center of each cheese. Brine was prepared with sodium chloride (PRS-codex, Panreac® Química SA, Barcelona, Spain) and distilled water.

### 2.2 Salting Operation

Salting treatment was carried out by using 25 % (w/w) sodium chloride brine at 4ºC. 72 cheese cylinders (30 mm diameter and 10 mm thick) were cut. Samples were immersed in a vessel containing the osmotic solution with continuous stirring, for 0, 10, 20, 30, 40, 50, 60, 90, 120, 180, 240, 360, 480, 720, 900 and 1440 min; later they were equilibrated in an isothermal chamber at 4ºC for 24 hours (equilibrated samples), in order to remove the water and salt profiles and estimate the sorption isotherm (relation between moisture and water activity in an isothermal and equilibrated system), following the methodology of Castro-Giraldez et al. (2010).

Mass was determined by using a Mettler Toledo Balance (± 0.0001 g) (Mettler-Toledo, Inc., USA). The surface water activity was determined by a dew point hygrometer Decagon (Aqualab® series 3TE) with precision ± 0.003. Also the water activity of the osmotic solution was measured at each osmotic time. Measurements were done in structured samples (not minced), thus the obtained $a_w$ is considered to be the surface $a_w$

(Velázquez-Varela et al., 2014). The analysis of water content was adapted from the method of AOAC (Method 934.06, 2000) where moisture of equilibrated samples were obtained by using a vacuum oven, 24 hours after the treatment, and moisture of non-equilibrated samples were estimated using weight balances. Two to three grams of grated cheese were accurately weighed into a tared tempered glass dish and the cheese spread into a uniform layer. The sample was placed in a vacuum oven at room temperature and the pressure in the oven reduced to 100 mbar. The temperature was then slowly increased to 65ºC, and the samples were maintained at this temperature for 14 d. The dried samples were then removed from the oven, cooled to room temperature in a desiccator, and weighed. The volume was determined by image analysis (Canon® Power Shot SX210 IS), using Adobe Photoshop® software (Adobe Systems Inc., San Jose, CA, USA) in order to determine the diameter and the thickness of the samples by a non-destructive method. Ion content was carried out by means of an ion chromatograph (Methrom Ion Analysis, Herisau, Switzerland), using an universal standard column (Metrosep C2–150, 4.0 x 150 mm) along with an eluent composed of tartaric acid (4.0 mmol/L) and dipicolinic acid (0.75 mmol/L), equipped with electronic detectors. In every case, the cheese samples were previously homogenized at 4200 rpm in an Ultraturrax T25 for 5 min and centrifuged (J.P. Selecta S.A., Medifriger-BL, Barcelona, Spain) at 8000 rpm for 20 min at 4ºC. Afterwards, 1 mL of supernatant was diluted with Milli®-Q water in a 250 mL Erlenmeyer flask. The clarified extract was filtered through a 0.45 μm Millipore filter; 15 mL was used to analyse the anion content. Measurements were made in duplicate.

### 2.3 Permittivity measurement

Permittivity was measured by using an Agilent 85070E Open-ended coaxial probe connected to an Agilent E8362B vector network analyser. The software of the network analyser calculates the dielectric constant and loss factor. The system was calibrated by

using three different types of loads: open circuit (air), short-circuit and 4°C distilled water. The dielectric properties were measured by attaching the probe to the surface of the samples at 4°C from 500 MHz to 20 GHz. The mean values of at least three replicates of the cheese samples are reported in this article.

### 2.4 Statistical analysis

Statistical analysis was carried out with the Statgraphic Centurion ®, version 16.2.04 (Statpoint Technologies, Inc, U.S.A.). Multiple regression factorial analyses were performed in order to find significant interaction among dielectric constant at 20 GHz with the number of water molecules and the water fluxes. Moreover, multiple regression factorial analyses were carried out in order to find significant interaction among conductivity at 0.5 GHz with the number of Calcium, Chloride, and Sodium molecules and the Sodium chloride fluxes.

## 3. **Results and Discussion**

Cheese samples were measured just after the salting treatment (non-equilibrated samples) and after 24 hours of repose (equilibrated samples). 24 hours of repose is considered enough time to reach the equilibrium in the whole sample, demonstrated by the salt profiles disappearance (Velázquez-Varela et al., 2014). During the repose time, samples were on disposable sample cups, closed with parafilm®, and preserved in an isothermal chamber in order to isolate the samples and to reach equilibrium. The salting process in brine produces a movement of ions ($Na^+$ and $Cl^-$) from the brine into the cheese, and simultaneously there is an outflow of water and calcium from the cheese to the solution, promoted by gradients of chemical potentials. In cheese, the mass water loss is higher than the amount of salt incorporated; as a result, there is a loss of weight in the cheese (Velázquez-Varela et al., 2014).

147 The desorption profiles of non-equilibrated samples and the desorption isotherms of
148 equilibrated samples were obtained in order to estimate the moisture of the surface ($x_w^{surf}$)
149 following the procedure described by Traffano-Schiffo et al., 2014 (see Figure 1) .
150 Surface water activity is a superficial measurement and moisture is an average value of
151 the whole sample, as was explained in the Material and Methods section. Equilibrated
152 samples did not have moisture profiles; therefore, equilibrated isotherm represents the
153 real relation between moisture and water activity. Thus, the equilibrated isotherm is an
154 excellent tool to obtain, with the surface water activity of non-equilibrated samples, the
155 surface moisture of those samples (samples with moisture profiles). In figure 1, it is also
156 possible to observe an increase in surface water activity caused by the internal fluxes that
157 occur in cheese during the repose time.
158 The water and salt fluxes were calculated as follows:

159 $$J_w^{0h} = \frac{-\Delta M_w^{0h} \cdot M_0}{\Delta t \cdot S \cdot Mr_w} \quad \text{(Equation 1)}$$

160 $$J_{NaCl}^{0h} = \frac{-\Delta M_{NaCl}^{0h} \cdot M_0}{\Delta t \cdot S \cdot Mr_{NaCl}} \quad \text{(Equation 2)}$$

161

162 Where, J is the flux (mol $s^{-1}$ $m^{-2}$), ΔM represents the mass variation (dimensionless), $M_0$
163 is the initial mass of the sample (g), Δt is the process time, S is the area of the sample
164 during treatment ($m^2$), Mr is the molecular weight of the compound (18 g $mol^{-1}$ for water
165 and 58.4 g $mol^{-1}$ for sodium chloride), and the subscripts "w" and "NaCl" represent water
166 and sodium chloride, respectively. The superscript "0h" represents the non-equilibrated
167 samples.
168 Figure 2 shows the water and NaCl molar fluxes. These fluxes decrease with time, caused
169 by a decrease of the engine of the transport (chemical potential) throughout the treatment
170 (Velázquez-Varela et al., 2014).

171 In order to understand the electric behaviours affected by water and ions molecules in the
172 sample surface, it is necessary to calculate its content in the surface. The surface water
173 mass fraction was calculated by using the surface water activity of non-equilibrated
174 samples, from the equilibrated isotherm. The surface sodium chloride mass fraction was
175 estimated by using the surface water activity following the model of Fito et al. (2011).
176 Figure 3 shows the evolution of the overall value of water mass fraction and the water
177 mass fraction in the surface, both expressed in liquid phase ($z_w$), throughout the salting
178 treatment (non-equilibrated samples).

179 In order to understand the permittivity, measured by a coaxial probe in contact with the
180 surface of the sample, it is necessary to know its penetration depth ($D_P$), which was
181 calculated as follows (Metaxas & Meredith, 1983):

182 $$D_P = \frac{\lambda_0}{2\pi\sqrt{2\varepsilon'}}\left[(1 + tan^2\delta)^{1/2} - 1\right]^{-1/2} \quad \text{(Equation 3)}$$

183 where $\boldsymbol{\lambda}_0$ is the wavelength, being 60 cm at 0.5 GHz and 1.5 cm at 20 GHz; tan δ is the
184 loss tangent ($\tan\delta = \frac{\varepsilon''}{\varepsilon'}$).

185 Figure 4 shows a scheme of cheese sample in contact with the microwave probe,
186 indicating the penetration depth of the electric field at 20 GHz and 0.5 GHz. At frequency
187 of 20 GHz the predominant effect is the γ-dispersion, explained as the induction and
188 orientation of the dipolar molecules. The most important dipolar molecule is water,
189 therefore water status can be studied in this spectral range. The two properties that
190 influence this dispersion are the number of water molecules and their mobility (Talens et
191 al., 2016, Traffano-Schiffo et al 2015). During the salting process, the microwave
192 penetration volume (MPV) reaches a minimum quantity of water molecules before the
193 rest of the sample volume; at this point, the dielectric signal will be affected by the loss
194 of water molecules. When the steady state is reached at the surface, the sample will

continue loosing water molecules from the rest of the sample volume, generating a water flux across the MPV, changing the mobility of the water molecules and, therefore, the water mobility has the major effect of the dispersion.

Figure 4 shows, at the bottom of the scheme, the effect at 500 MHz. Ionic conductivity is the major contribution to the dielectric losses. Ionic conductivity does not affect the electric storage because no molecular orientation occurs by the electric field. The conductivity value changes with the quantity and mobility of the electrolytes (chloride, sodium and calcium). The penetration index reaches the whole sample, indicating an average value of the state of the ions. The saturation value of the liquid phase is rapidly reached, taking a constant value of the ions molecules. Nevertheless, the fluxes of water and calcium maintain the fluxes of sodium and chloride (Velázquez-Varela et al., 2014), changing the value of conductivity.

Figure 5 shows the dielectric constant and the loss factor spectra of the samples just after the salting treatment. It is also important to analyse the water molecules in the sample surface by dielectric spectroscopy. For this purpose, there were calculated the number of water and ions molecules by using the surface mass fraction in the case of water, and the ions mass fraction of the sample in the case of ions (Equation 4).

$$N_j = \frac{X_j \ N_A}{M_{r_j}} \qquad \text{(Equation 4)}$$

where: N represents the molecules (molecules·$g_{dm}^{-1}$), $X_j$ is the surface moisture expressed by solid matrix (neither water nor ions) in the case of water ($g_w \cdot g_{SM}^{-1}$) and ion mass fraction (sodium, calcium and chloride) expressed by solid matrix (neither water nor ions) in the case of ions ($g_i \cdot g_{SM}^{-1}$), $N_A$ is the Avogadro constant ($6.022 \cdot 10^{23}$ $mol^{-1}$) and $M_r$ is the molecular weight, being 18 g·$mol^{-1}$ for water, 22.99 g·$mol^{-1}$ for sodium, 40.08 g·$mol^{-1}$ for calcium and 35.45 g·$mol^{-1}$ for chloride.

The interaction of the electric field with cheese in γ-dispersion is affected by the amount of water molecules and its motion. Multiple regression factorial analyses were made in order to find significant interaction amongst the dielectric constant at 20 GHz with the number of water molecules and the water fluxes throughout the salting treatment. This analysis showed that the relation between dielectric constant at 20 GHz and the number of water molecules is significant ($p<0.05$) until the surface saturation phenomena of cheese liquid phase, i.e. during the first 180 minutes of treatment. The analysis also showed that there exists a very significant ($p<0.01$) relation between the dielectric constant at 20 GHz and the water flux from 90 minutes until the end of the treatment. Figure 6 presents the relation between the dielectric constant at 20 GHz and the number of the surface water molecules in non-equilibrated samples. It is possible to observe that there exists a linear relationship between both variables at the beginning of the salting treatment as was explained before; thus, the surface water molecules can be obtained by measuring the dielectric constant at 20 GHz when the surface is in an unsteady state. When the system reaches the steady state on the surface, the amount of water molecules is constant but the water is still flowing throughout this volume, coming from the middle of the samples and changing the motion of the water molecules in the microwave penetration volume. Therefore, the capability of water molecules to be induced and orientated changes with this water flux. In figure 7, it is possible to observe that the dielectric constant at 20 GHz is related very significantly ($p<0.01$) with the water flux after 90 minutes of treatment, at which the steady state is reached by the system. Therefore, the dielectric model to predict water losses has to be non-linear, explaining not only the water losses in the microwave penetration volume, but also in the overall product, because when the penetration microwave volume reaches the steady state, the model predicts the water flux.

244 The conductivity of the sample (σ) was calculated at 0.5 GHz as follows:

245 $$\sigma = \varepsilon'' \varepsilon_0 \omega \quad \text{(Equation 5)}$$

246 where: ω is the angular frequency and the $\varepsilon_0$ is the dielectric constant in vacuum
247 ($\varepsilon_0$=8.8542 $10^{-12}$ F·$m^{-1}$).

248 The conductivity at 0.5 GHz was represented with regard to the amount of ions molecules
249 of the sample estimated by equation 4 (Figure 8). It is important to highlight that, at this
250 frequency, the microwave penetration depth covers most of the sample; thus, the
251 conductivity can be considered an overall value of the whole sample.

252 In figure 8, at first 60 minutes of salting, a linear relation between the accumulation of
253 the electrolytic molecules and ionic conductivity can be appreciated, being very
254 significant ($p<0.01$). When saturation is achieved in the liquid phase, the conductivity
255 decreases. So, in the first period (the first 60 minutes) conductivity changes very
256 significantly with the accumulation of electrolyte molecules, but from this time it is no
257 longer significant.

258 After 60 minutes, when the relation between the conductivity and the accumulation of
259 electrolyte molecules is non significant, the conductivity begins to decrease. This
260 decrease is promoted by a decrease in the mobility of the electrolytic molecules in the
261 liquid phase, sodium, chloride and calcium. The cause of mobility in this period of salting
262 is the motion produced by the ion fluxes, where the fluxes are induced by the absorption
263 of sodium and chloride ions in the casein matrix and by the loss of calcium from the
264 casein structure (Velázquez-Varela et al., 2014). In Figure 9 it can be observed, after 60
265 minutes, a very significant ($p<0.01$) linear relationship between the sodium chloride flux
266 and the ionic conductivity until the end of the process. Therefore, it is possible to predict

the level of salting and thus the structural changes in the casein with the measurement of the conductivity at 500 MHz

## 4. Conclusions

The non-linear model proposed by using the dielectric constant at 20 GHz explains not only the water losses in the MPV, but also in the overall product, because when the MPV reaches the steady state, the model predicts the water flux. In case of salting prediction, the ionic conductivity estimated at 500 MHz explains the level of salting, and for bigger samples, the variable can also be explained, because it is related not only to the accumulation of the electrolyte molecules, but also to the fluxes.

Therefore, coupled measurements of dielectric properties at 20 GHz and 500 MHz can predict the chemical species involved in cheese salting process, and its structural changes.

## 5. Acknowledgements

The authors acknowledge the financial support from the Spanish Ministerio de Economía, Industria y Competitividad, Programa Estatal de I+D+i orientada a los Retos de la Sociedad AGL2016-80643-R. Author J. Velázquez-Varela thanks the Consejo Nacional de Ciencia y Tecnología (CONACyT) of México for their support. This paper was published under the frame of European Social Fund, Human Resources Development Operational Programme 2007-2013, project no. POSDRU/159/1.5/S/132765.

## 6. References

Ahmed, J., Ramaswamy, H. S., & Raghavan, V. G. S. (2007). Dielectric properties of butter in the MW frequency range as affected by salt and temperature. *Journal of Food Engineering*, 82, 351-358.

AOAC, 2000. AOAC, Official Methods of Analysis (17th ed.) Association of Official Analytical Chemists, Arlington, VA (2000).

Ball, J. A. R., Horsfield, B., Holdem, J. R., Keam, R. B., Holmes, W. S., & Green, A. (1996). Cheese curd permittivity and moisture measurement using a 6-port reflectometer. In Asia Pacific Microwave Conference, New Delhi.

Castro-Giráldez, M., Fito, P.J., & Fito, P. (2010). Application of microwaves dielectric spectroscopy for controlling pork meat (*Longissimus dorsi*) salting process. *Journal of Food Engineering*, 97, 484-490.

Cevoli, C., Ragni, L., Gori A., Berardinelli A., & Fiorenza C. M. (2012). Quality parameter assessment of grated Parmigiano-Reggiano cheese by waveguide spectroscopy. *Journal of Food Engineering*, 113, 201-209.

Chevalier, D., Ossart, F., & Ghommidh, C. (2006). Development of a nondestructive salt and moisture measurement method in salmon (Salmo salar) fillets using impedance technology. *Food Control*, 17, 342–347.

Dickinson, E., & Miller, R. (2001). Food Colloids: Fundamentals of Formulation. The Royal Society of Chemistry, UK.

Everard, C.D., Fagan, C.C., O'Donell, C.P., O'Calleghan, D.J., & Lyng, J.G. (2006) Dielectric properties of process cheese from 0,3 to 3 GHz. *Journal of Food Engineering*, 75, 415-422

Fito, P, Fito, P.J, Betoret, N., Argüelles A. & Chenoll, C. (2011) Thermodynamic approach to equilibrium isotherms in salted structured food. *Journal of Food Process Engineering*, 34, 623–638

Floury, J., Camier, B., Rousseau, F., Lopez, C., Tissier, J. P., & Famelart, M. H. (2009). Reducing salt level in food: Part 1. Controlled manufacture of model cheese systems and their structure-texture relationships. *LWT – Food Science and Technology*, 42, 1611–1620.

315 Fox, P.F., O'Connor, T.P., McSweeney, P.L.H., Guinee, T.P., & O'Brien, N.M. (1996).
316 Cheese: physical, biochemical, and nutritional aspects. Advances. *Food Nutrition*
317 *Research*, 39, 163-328.

318 Green, A. D. (1997). Measurements of the dielectric properties of Cheddar cheese.
319 *Journal of Microwave Power and Electromagnetic Energy*, 32, 16–27.

320 Herve, A. G., Tang, J., Luedecke, L., & Feng, H. (1998). Dielectric properties of cottage
321 cheese and surface treatment using microwaves. *Journal of Food Engineering*, 37, 309–
322 410.

323 Kubiš, I., Krivanek, I., & Gajdusek, S. (2001). The relationships between the chemical,
324 dielectric and sensory properties of Edam cheese during ripening. Czech *Journal of Food*
325 *Science*, 19, 85–89.

326 Mamdouh, E.B. (2012). Salt in Cheese: A Review. *Current Research in Dairy Sciences*,
327 4, 1-5.

328 Metaxas A. C. & Meredith R. J. (1993). Industrial Microwave Heating. UK: IEE Power
329 Engineering Series 4. Peter Peregrinus Ltd. (Chapter 2 and 4)

330 Mohiri, A., Burhanudin, A. Z., & Ismail, I. (2011). Dielectric Properties of Slaughtered
331 and Non-slaughtered Goat Meat. In IEEE International RF and Microwave Conference.
332 Malaysia.

333 Nelson, S.O. & Datta, A.K. (2001). Dielectric properties of food materials and electric
334 field interactions. In A.K. Datta & R.C. Anantheswaran (Eds), *Handbook of Microwave*
335 *Technology for Food Applications*. New York: Marcel Dekker Inc.

336 Payne, M.R., & Morison, K.R. (1999). A multi-component approach to salt and water
337 diffusion in cheese. *International Dairy Journal*, 9, 887–894.

338 Schwan, H. P. 1988. Dielectric spectroscopy of biological cells, *Special Issue on*
339 *Electricity and Biophysics, Ferroelectrics*, 86, 205-223.

340 Shiinoki, Y., Motouri, Y. & Ito. K. (1998). On-line Monitoring of Moisture and Salt
341 Contents by the Microwave transmission Method in a Continuous Salted Butter-making
342 Process. *Journal of Food Engineering*, 38, 153-167.

343 Smith, J., Carr, A., Goldinga, M., Reid, D., & Zhang, L. (2011) Assessing the use of
344 dielectric spectroscopy to analyse calcium induced compositional and structural changes
345 in a model cheese. Selection of 11th International Congress on Engineering and Food
346 (ICEF11). *Proceedings Food Science*, 1, 1833 – 1840

347 Talens, C., Castro-Giraldez, M., Fito, P.J. (2016). Study of the effect of microwave power
348 coupled with hot air drying on orange peel by dielectric spectroscopy. *LWT-Food Science*
349 *and Technology*, 66, 622-628

350 Traffano-Schiffo, M.V., Castro-Giraldez, M., Fito P.J., Balaguer, N. (2014).
351 Thermodynamic model of meat drying by infrarred thermography. *Journal of Food*
352 *Engineering*, 128, 103-110

353 Traffano-Schiffo, M.V., Castro-Giraldez, M., Colom, R.J., Fito P.J. (2015). Study of the
354 application of dielectric spectroscopy to predict the water activity of meat during drying
355 process. *Journal of Food Engineering*, 166, 285-290

356 Velázquez-Varela, J., Fito, P.J. & Castro-Giráldez, M. (2014). Thermodynamic analysis
357 of salting cheese process. *Journal of Food Engineering*, 130, 36-44.

358 Venkatesh, M.S. & Raghavan, G.S.V. (2004). An Overview of Microwave Processing
359 and Dielectric Properties of Agri-food Materials. *Biosystems Engineering*, 88, 1-18

360 Walstra, P., Wouters, J. T. M. & Geurts, T. J. (2006). Dairy science and technology. (2nd
361 ed.). Florida: Taylor & Francis Group, LLC.

362 Wang, S., Tang, J., Johnson, J. A., Mitcham, E., Hansen J. D., Hallman, G., Drake, S.R,
363 & Wang, Y. (2003). Dielectric Properties of Fruits and Insect Pests as related to Radio
364 Frequency and Microwave Treatments. *Biosystems Engineering*, 85, 201–212.

365

366

## FIGURE CAPTION

Figure 1. Desorption profile of non-equilibrated (●) and desorption isotherm of equilibrated (♦) samples.

Figure 2. Evolution of water (■) and NaCl (♦) fluxes throughout the osmotic treatment.

Figure 3. Evolution of the surface water mass fraction in the liquid phase with regard to the treatment time, where: (▲) represents the value of the sample surface and (●) represents the overall value.

Figure 4. Scheme of the dielectric properties measurements of cheese samples throughout the salting treatment.

Figure 5. Evolution of the dielectric constant and loss factor spectra of the samples throughout the treatment (non-equilibrated samples), where: (─) 0 min; (— ) 10 min; (- - -) 20 min; (· · ·) 30 min; (⋯) 40 min; (— ) 50 min; (– – –) 60 min; (· · ·) 90 min; (⋯) 2 h; (—) 3 h; (– – –) 4 h; (· · ·) 6 h; (⋯) 8 h; (- · - · -) 12 h; (– · – · –) 15 h; (– · – · – · –) 24 h.

Figure 6. Relation of the dielectric constant at 20 GHz with regard to the number of surface water molecules in solid matrix throughout the salting treatment.

Figure 7. Evolution of the water flux with regard to the dielectric constant at 20 GHz.

Figure 8. Conductivity at 0.5 GHz with regard to the amount of ions molecules of the sample.

Figure 9. Flux of sodium chloride with regard to conductivity.

Wang, S., Tang, J., Johnson, J. A., Mitcham, E., Hansen J. D., Hallman, G., Drake, S.R, & Wang, Y. (2003). Dielectric Properties of Fruits and Insect Pests as related to Radio Frequency and Microwave Treatments. *Biosystems Engineering*, 85, 201–212.

## FIGURE CAPTION

Figure 1. Desorption isotherm of non-equilibrated (●) and equilibrated (♦) samples.

Figure 2. Evolution of water (■) and NaCl (♦) fluxes throughout the osmotic treatment.

Figure 3. Evolution of the surface water mass fraction in the liquid phase with regard to the treatment time, where: (▲) represents the value of the sample surface and (●) represents the overall value.

Figure 4. Scheme of the dielectric properties measurements of cheese samples throughout the salting treatment.

Figure 5. Evolution of the dielectric constant and loss factor spectra of the samples throughout the treatment (non-equilibrated samples), where: (─) 0 min; (— ) 10 min; (- - -) 20 min; (· · ·) 30 min; (···) 40 min; (— ) 50 min; (- - -) 60 min; (· · ·) 90 min; (···) 2 h; (—) 3 h; (- - -) 4 h; (· · ·) 6 h; (· · ·) 8 h; (- · - · -) 12 h; (- · - · -) 15 h; (- · - · -) 24 h.

Figure 6. Relation of the dielectric constant at 20 GHz with regard to the number of surface water molecules in solid matrix throughout the salting treatment.

Figure 7. Evolution of the water flux with regard to the dielectric constant at 20 GHz.

Figure 8. Conductivity at 0.5 GHz with regard to the amount of ions molecules of the sample.

Figure 9. Flux of sodium chloride with regard to conductivity.

**Figure 1**

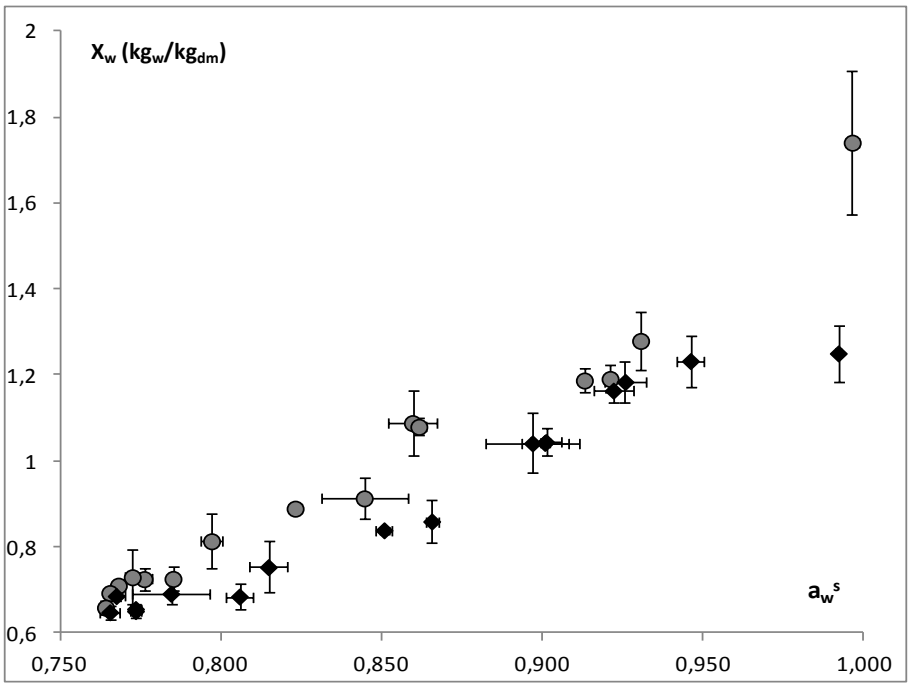


Figure 1.

**Figure 2**

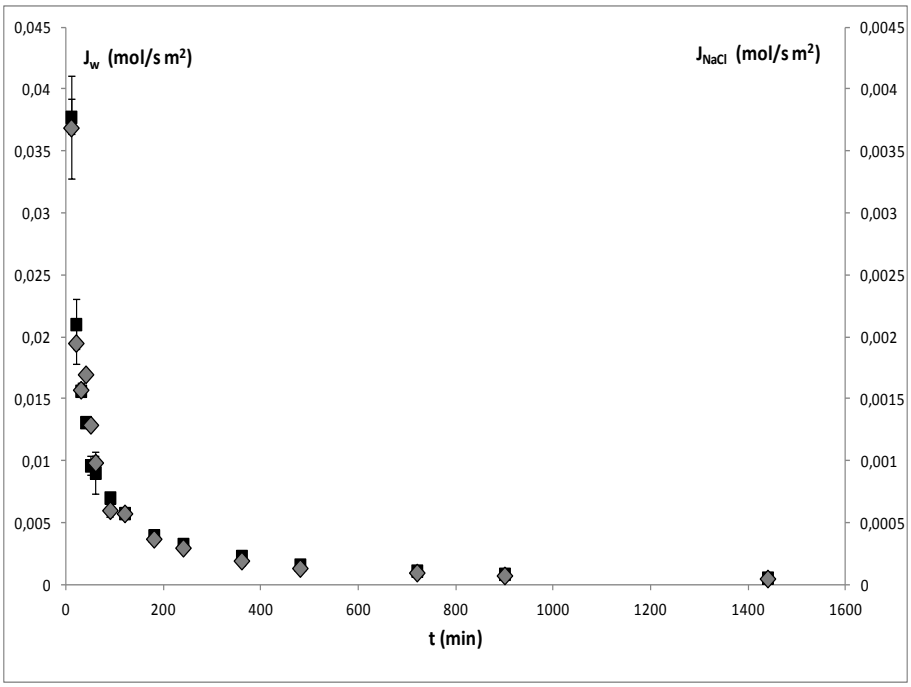


Figure 2.

**Figure 3**

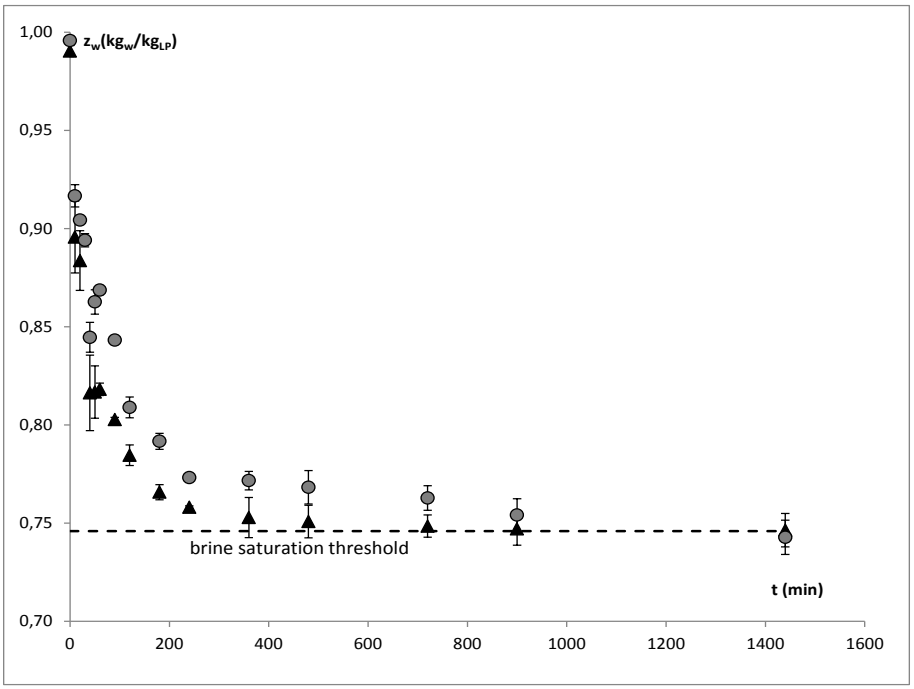


Figure 3.

**Figure 4**

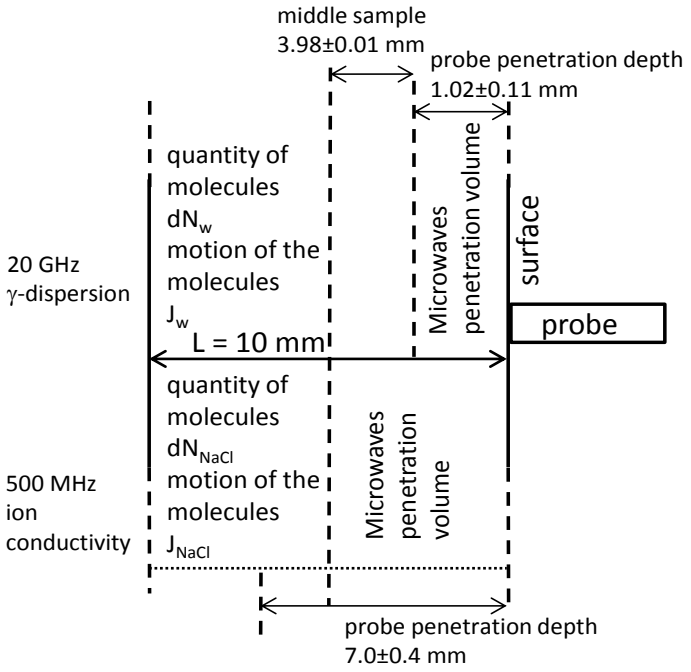


Figure 4.

**Figure 5**

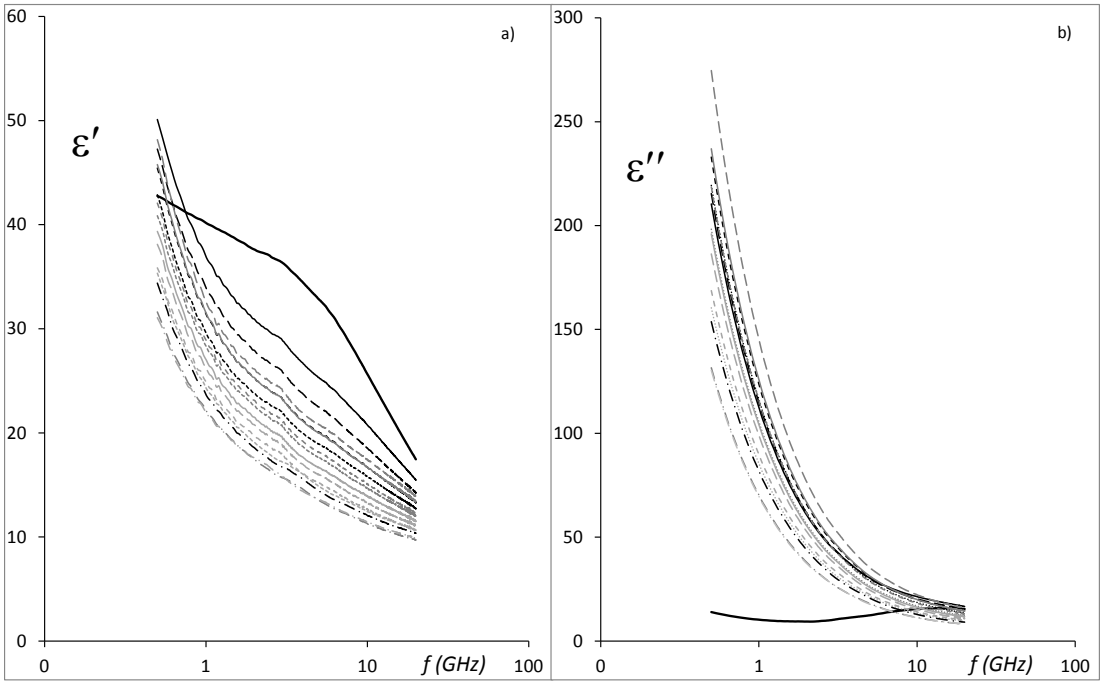


Figure 5.

**Figure 6**

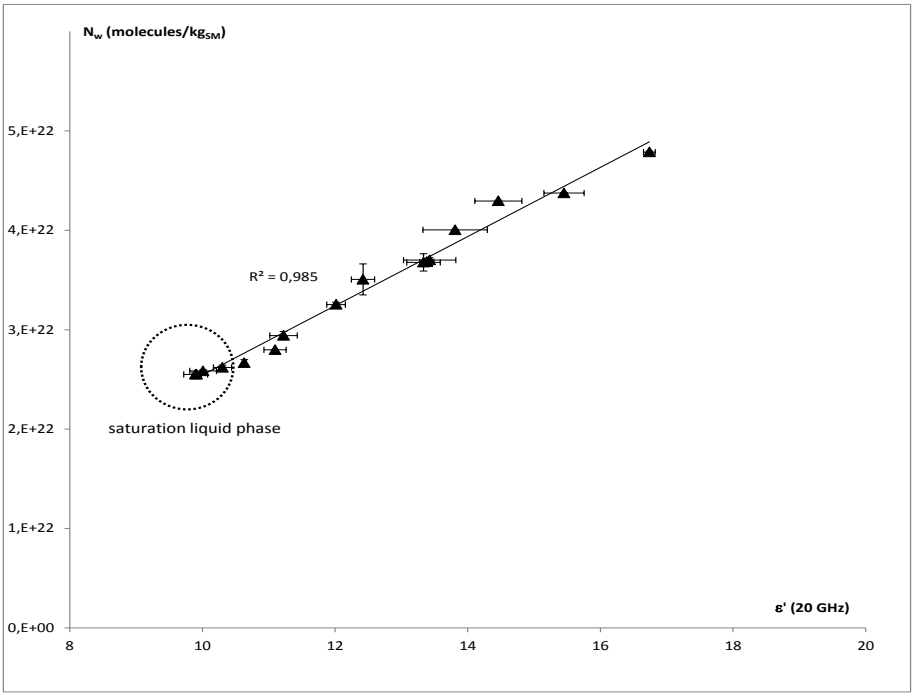


Figure 6.

**Figure 7**

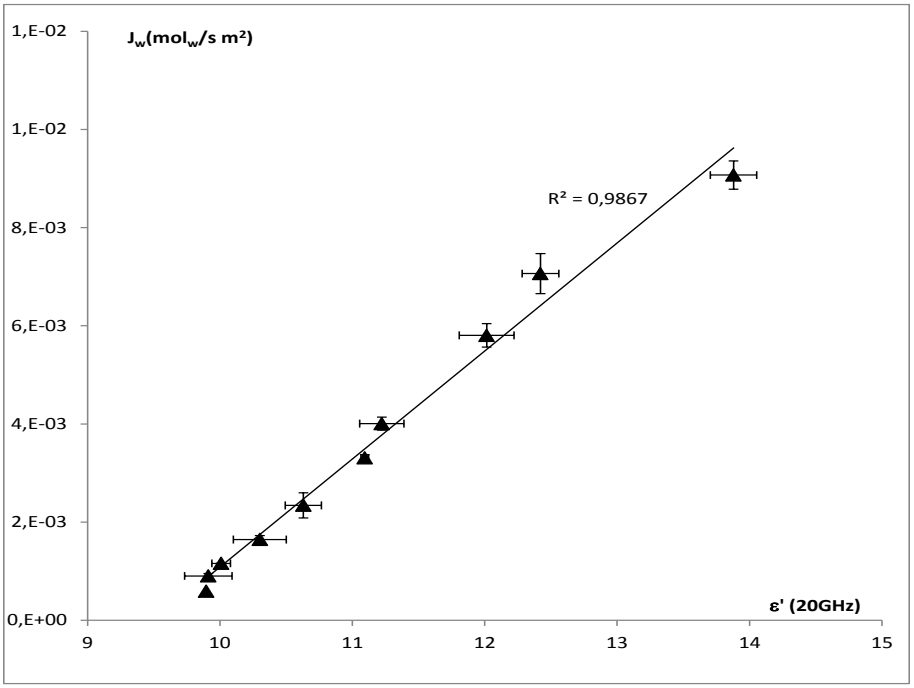


Figure 7.

**Figure 8**

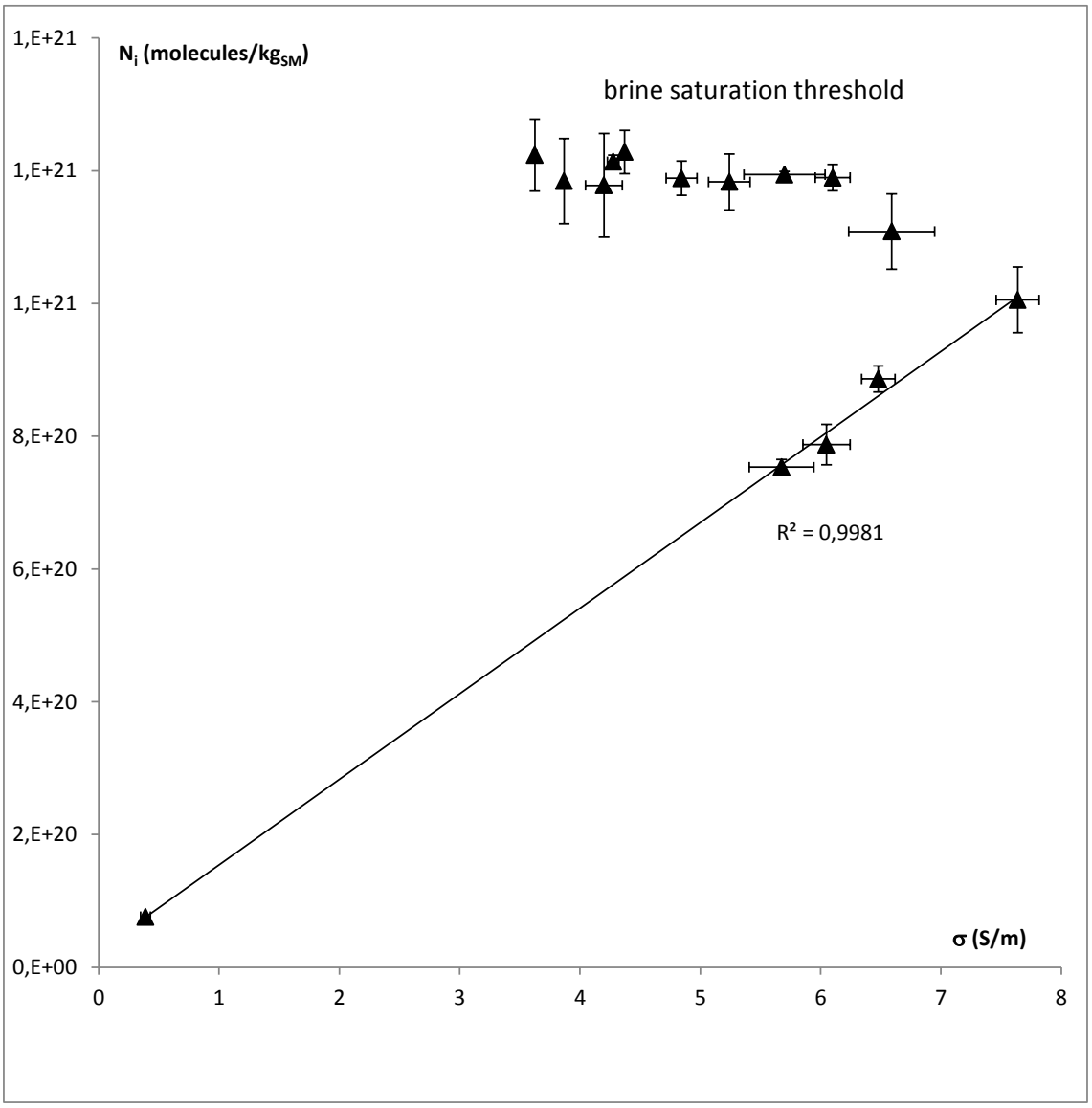


Figure 8.

**Figure 9**

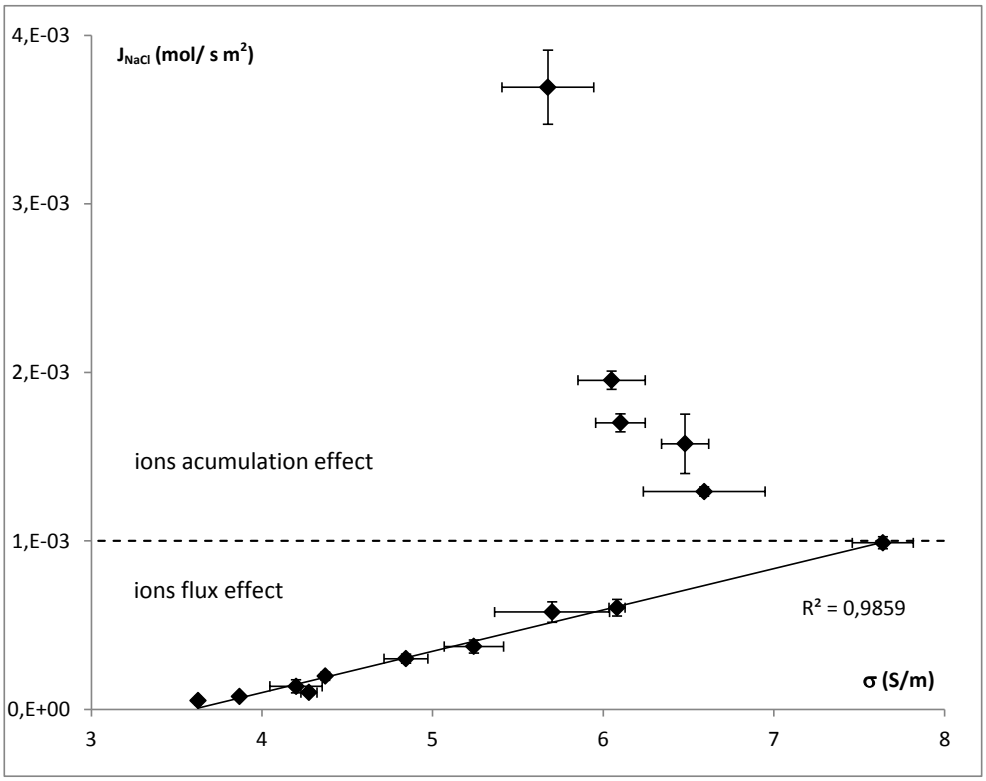


Figure 9.

## FIGURE CAPTION

Figure 1. Desorption isotherm of non-equilibrated (●) and equilibrated (♦) samples.

Figure 2. Evolution of water (■) and NaCl (♦) fluxes throughout the osmotic treatment.

Figure 3. Evolution of the water mass fraction in the liquid phase with regard to the treatment time, where: (▲) represents the value of the sample surface, and (●) represents the overall value.

Figure 4. Scheme of the dielectric properties measurements of cheese samples throughout the salting treatment.

Figure 5. Evolution of the dielectric constant and loss factor spectra of the samples throughout the treatment (non-equilibrated samples), where: (─) 0 min; (— ) 10 min; (- - -) 20 min; (- · ·) 30 min; (···) 40 min; (— ) 50 min; (- - -) 60 min; ( · ·) 90 min; (···) 2 h; (—) 3 h; (- - -) 4 h; ( · ·) 6 h; ( · ·) 8 h; (- · - · -) 12 h; (- · - · -) 15 h; (- · - · -) 24 h.

Figure 6. Relation of the dielectric constant at 20 GHz with regard to the number of surface water molecules in solid matrix throughout the salting treatment.

Figure 7. Evolution of the water flux with regard to the dielectric constant at 20 GHz.

Figure 8. Conductivity at 0.5 GHz with regard to the amount of ions molecules of the sample.

Figure 9. Flux of sodium chloride with regard to the conductivity.